



Published in final edited form as:

ACS Appl Bio Mater. 2020 February 17; 3(2): 859–868. doi:10.1021/acsabm.9b00944.

Injectable Highly Tunable Oligomeric Collagen Matrices for Dental Tissue Regeneration

Divya Pankajakshan,

Indiana University School of Dentistry, Indianapolis, Indiana

Sherry L. Voytik-Harbin,

Purdue University, West Lafayette, Indiana

Jacques E. Nör,

University of Michigan School of Dentistry, Ann Arbor, Michigan

Marco C. Bottino

University of Michigan School of Dentistry, Ann Arbor, Michigan

Abstract

Current stem cell transplantation approaches lack efficacy, because they limit cell survival and retention and, more importantly, lack a suitable cellular niche to modulate lineage-specific differentiation. Here, we evaluate the intrinsic ability of type I oligomeric collagen matrices to modulate dental pulp stem cells (DPSCs) endothelial and odontogenic differentiation as a potential stem cell-based therapy for regenerative endodontics. DPSCs were encapsulated in low-stiffness (235 Pa) and high-stiffness (800 Pa) oligomeric collagen matrices and then evaluated for long-term cell survival, as well as endothelial and odontogenic differentiation following in vitro cell culture. Moreover, the effect of growth factor incorporation, i.e., vascular endothelial growth factor (VEGF) into 235 Pa oligomeric collagen or bone morphogenetic protein (BMP2) into the 800 Pa oligomeric collagen counterpart on endothelial or odontogenic differentiation of encapsulated DPSCs was investigated. DPSCs-laden oligomeric collagen matrices allowed long-term cell survival. Real time polymerase chain reaction (RT-PCR) data showed that the DPSCs cultured in 235 Pa matrices demonstrated an increased expression of endothelial markers after 28 days, and the effect was enhanced upon VEGF incorporation. There was a significant increase in alkaline phosphatase (ALP) activity at Day 14 in the 800 Pa DPSCs-laden oligomeric collagen matrices, regardless of BMP2 incorporation. However, Alizarin S data demonstrated higher mineralization by Day 21 and the effect was amplified in BMP2-modified matrices. Herein, we present key data that strongly support future research aimed at clinical translation of an injectable oligomeric collagen system for delivery and fate regulation of DPSCs to enable pulp and dentin regeneration at specific locations of the root canal system.

Keywords

injectable; hydrogel; oligomeric collagen; regeneration; dental pulp; angiogenesis

Corresponding Author Phone: +1-734-763-2206; mbottino@umich.edu; Fax: +1-734-936-1597.

The authors declare no competing financial interest.

INTRODUCTION

In dentistry, the treatment of pulpal necrosis due to caries or trauma,¹ especially in immature permanent teeth, remains a clinical challenge, because the dental roots are thin and short, which consequently increase the risk of tooth fracture upon secondary trauma.² Besides playing a key role in tooth development, the dental pulp functions as a protective organ that can detect variations in temperature, pressure, or trauma.³ For these reasons, numerous investigators are exploring novel matrices and/or strategies for pulp-dentin regeneration directed toward extending the lifetime of permanent teeth.⁴⁻¹⁰

The development of injectable matrices for use in full-length root canals that supports cell growth, vascularization, and dentin formation is a key step toward clinically feasible pulp regeneration. Natural and synthetic hydrogels, nanofibers, nanoassemblies, and microspheres are being evaluated by investigators for pulp regeneration. Customized self-assembling peptide hydrogels consisting of “multidomain peptides” incorporating growth factors and dental pulp stem cells (DPSCs) induced the formation of vascularized soft connective tissue resembling dental pulp.⁹ Prevascularized constructs containing co-cultured DPSCs and endothelial cells embedded within PuraMatrix, which is a self-assembling peptide hydrogel, demonstrated enhanced in vivo neovascularization and osteodentin formation.⁴ Gelatin methacryloyl hydrogels with tunable physical and mechanical properties and ability for prevascularization is another recent strategy adopted for pulp regeneration.⁵ Scaffolds made of alginates and chitosan have also demonstrated promising results for their odontogenic differentiation capabilities. Alginate and nanohydroxyapatite composite scaffolds induced mineralization and differentiation of human DPSCs in vitro.¹¹ Porous chitosan–calcium–aluminate scaffolds in combination with a bioactive dosage of 1 α ,25-dihydroxyvitamin D3 enhanced the odontogenic potential of dental pulp cells in vitro.¹²

Meanwhile, nanostructured multilayered nanoassemblies and microspheres are other promising approaches to promote dental pulp tissue regeneration. Nanostructured and functionalized multilayered polyelectrolyte films of poly L-lysine dendrigraft, containing polyglutamic acid- α -melanocyte stimulating hormone were proposed to decrease inflammation and promote tissue regeneration in the pulpal space.¹³ Type I collagen-surface modified PLGA microspheres enhanced cell proliferation and odontogenic differentiation of dental pulp cells in vitro.¹⁴

Collagen is one of the most widely used injectable natural biomaterial, because of its excellent biocompatibility and easy tissue integration following degradation, and by their ability to act as a vehicle for growth factors.¹⁵ DPSC-encapsulated commercially available rhCollagen hydrogel transplanted to full-length root canals demonstrated improved organization of the newly formed pulp tissue.¹⁰ Collagen scaffolds incorporated with chemotactic factors, stromal cell-derived factor 1 α and bFGF, led to recruitment of stem/progenitor cells from adult dental pulp.¹⁶ Collagen gels also have been observed to support vasculogenesis and cell survival of endothelial colony forming cells in the presence of platelet releasate.¹⁷ However, a major limitation of present-day commercial polymerizable monomeric collagens is their inconsistent fibril density, because of the monomeric nature

that varies with every batch, thus making it difficult to predict their mechanical behavior and overall cell function.^{18,19} To that end, the fabrication of collagen-fibril matrices with tunable and highly reproducible fibril microstructures and biophysical properties (e.g., stiffness) is critical to guiding cell-matrix interactions. Recent research has focused on tailoring the stiffness and microstructure of collagen matrices by modulating collagen concentration (fibril density) and the oligomer:monomer ratio (extent of interfibril connectivity). Indeed, the cell-instructive properties of these matrices were unveiled when endothelial progenitor cells cultured on low-stiffness oligomeric collagens induced more extensive and persistent endothelial vessel networks, compared to monomeric matrices with identical stiffness.²⁰

In the current study, we hypothesized that the collagen matrix with low stiffness (235 Pa) would induce endothelial differentiation of DPSCs and the presence of a vascular endothelial growth factor (VEGF) would enhance this differentiation, and the collagen matrix with higher stiffness (800 Pa) would induce osteogenic differentiation and the presence of bone morphogenetic protein-2 (BMP2) would enhance the odontogenic/osteogenic differentiation of DPSCs. VEGF is a prototypic proangiogenic factor, and BMP2 is an osteoinductive protein; these respective compounds have been proven to play a vital role in inducing endothelial²¹ and osteogenic differentiation²² of mesenchymal stem cells. Thus, herein, we first determined the initial cell adhesion and spreading, long-term survival, and differentiation ability of DPSCs within unique oligomeric collagen matrices of precise stiffness. In addition, we investigated whether the incorporation of VEGF into the low-stiffness oligomeric collagen matrix or BMP2 into the high-stiffness counterpart would further amplify endothelial or odontogenic differentiation of encapsulated DPSCs, respectively. The uniqueness of our innovative strategy, i.e., DPSCs transplantation using a stiffer matrix along with BMP2 (dentin formation) or within a more compliant matrix containing VEGF (pulp regeneration), when concentrically injected into the root canal (Figure 1), carries a strong translational potential as a single-cell population could be used to target both endothelial and odontogenic differentiation as a stem cell-based therapy for regenerative endodontics.

MATERIALS AND METHODS

Cell Culture.

Human DPSCs isolated from adult third molars (Lonza) were cultured in DPSC complete medium (DPSCM) containing α -MEM (Sigma), 10% FBS (Atlanta Biologicals), and antibiotics (100 U/mL penicillin and 100 μ g/mL streptomycin). Cells were maintained in a humidified environment of 5% CO₂ at 37 °C, and the culture medium was changed every other day. DPSCs were passaged at confluency and passages 3–6 were used for the experiments.

Preparation of DPSC, VEGF, and BMP2 Encapsulated Oligomeric Collagen Matrices.

Type I oligomeric collagen was derived from the dermis of market-weight pigs, as previously described.²³ The oligomer was dissolved in 0.01 N hydrochloric acid (HCl) and standardized based on molecular composition and polymerization capacity, according to ASTM International Standard F3089-14.²⁴ Here, the polymerization capacity refers to the

relationship (polynomial function) between the shear storage modulus (G' , in units of Pa) of the self-assembled matrix and the oligomer concentration. Matrix stiffness values of collagen matrices prepared at oligomer concentrations of 1.37 and 2.88 mg/mL are given as shear storage moduli (G' , in units of Pa). To achieve matrices of defined fibril density and matrix stiffness, stock oligomer was diluted in 0.01 N HCl to a final concentration of 1.37 mg/mL (235 Pa) for endothelial differentiation, and 2.88 mg/mL (800 Pa) for odontogenic differentiation, and neutralized with a proprietary 10X self-assembly reagent prior to DPSCs encapsulation (1×10^6 cells/mL). To prepare GF-modified oligomeric collagen matrices, VEGF165 (50 ng/mL, Invitrogen) and BMP2 (50 ng/mL, Invitrogen) were added to collagen solutions before polymerization. To induce differentiation, endothelial growth medium (EGM) containing growth supplements and 2% FBS (EGM-2 Bullet Kit, Lonza) and an hMSC osteogenic differentiation medium (Lonza) containing dexamethasone, ascorbate, and β -glycerophosphate were used, respectively. The following approaches were evaluated (see Figure 2).

Simulated Growth Factor Release from Oligomeric Collagen Matrices.

Fluorescein isothiocyanate (FITC)-labeled dextran with molecular weight (M_w) of 40 000 and 20 000 were used as model drugs to simulate the M_w values of VEGF and BMP2, respectively. The distinct oligomeric collagens (235 and 800 Pa) were prepared (100 μ L), modified with 500 μ g Dextran ($M_w = 40\ 000$ or $20\ 000$), and then pipetted into each well of a 96-well plate. Media (200 μ L) was then added to each well. The constructs were incubated at 37 °C and 5% CO₂ for 14 days and 100 μ L of medium was collected from each well at distinct time points up to 14 days, while maintaining the incubation volume constant by replacing the withdrawn amount with fresh medium. Fluorescence intensity was measured (Synergy HTX Microplate Reader, Biotek) using excitation and emission wavelengths of 485 and 520 nm, respectively. The results were compared to the amount of simulated GFs released when similarly incorporated into a commercially available hydrogel (PuraMatrix) prepared at concentrations of 0.20% and 0.25% ($n = 5$).

Cell Morphology.

Cell morphology within the oligomeric collagen matrices was evaluated by confocal microscopy after staining the actin cytoskeleton (rhodamine-phalloidin, Molecular Probes) and nuclei (SYTO 13, Molecular Probes) 24 h and 72 h post-culture ($n = 3$). Briefly, 1×10^6 cells were suspended in 1 mL of oligomeric collagen solution and 200 μ L of the suspension was allowed to polymerize in each well of an 8-well slide (Lab-Tek Permanox chamber slide; Thermo Scientific). To each well, 200 μ L of medium was added for cell culture. At each time point, cells were fixed with 3.7% paraformaldehyde in PBS for 30 min at room temperature (RT) and permeabilized for 10 min with 0.1% Triton X-100. F-actin was stained using rhodamine-phalloidin (1:1000 dilution) for 30 min and nuclei was stained using SYTO 13 (10 min; 1:1000 dilution). Images were captured using a confocal/2-photon Olympus FV1000 MPE system (Olympus America), using a XLUMPLFL20XW objective with a numerical aperture (NA) of 0.95. The images presented are maximum intensity projections of Z-slices (depth of $\sim 300\ \mu$ m). Rhodamine phalloidin and SYTO 13 have excitation and emission at 540/565 and 488/509 nm, respectively.

Cell Survival.

Cell survival within the oligomeric collagen matrices was investigated using CellTiter 96 AQueous One Solution Reagent (Promega). The cells were encapsulated in the oligomeric collagen matrices at a density of 10^6 cells/mL and 150 μL collagen-DPSC solution was added to each well of a 96-well plate to form constructs and 150 μL of media was used for culture. Cell proliferation was assessed on Days 1, 3, 7, 14, and 21. At each time point, 150 μL of the reagent–media mixture (5:1) was added to each well and incubated for 3 h at 37 °C and 5% CO_2 . After incubation, 100 μL of the mixture was pipetted to each well of a 96-well plate and the absorbance at 490 nm was recorded, using a microplate reader (Biotek).

Endothelial Differentiation.

DPSCs-laden oligomeric collagen matrices ($\sim 10^6$ cells/mL) were cultured in 24-well plates containing DPSCM or EGM for 1, 3, 7, 14, 21, and 28 days. Total RNA from constructs was extracted using TRIzol reagent.¹⁸ Real-time polymerase chain reaction (PCR) was performed to determine the expression of selected endothelial markers, von Willebrand Factor (vWF), platelet endothelial cell adhesion molecule 1 (PECAM-1), and vascular endothelial (VE)-cadherin using primers that were designed using the Primer quest tool (IDT) (see Table 1). RNA yield was quantified using a Take3 plate (Biotek) and cDNA was synthesized using Improm II reverse transcription kit (Promega) with 1 μg of total RNA as a template, 5 \times reaction buffer, MgCl_2 , dNTP mix, RNase inhibitor, and Improm-II reverse transcriptase.

Real-time PCR was performed using 8 μL cDNA, 10 μL iQSYBR green PCR Master Mix (Bio-Rad Laboratories), and 25 pmol/ μL of forward and reverse primers (Integrated DNA Technologies) using a CFX96 Real-time PCR (BioRad) ($n = 3$). The PCR cycling conditions were 5 min at 95 °C for initial denaturation, followed by 40 cycles of 30 s at 95 °C, 30 s at 53 °C (depending on the primer annealing temperatures) and 30 s at 72 °C (see Table 1). Specificity of the primers was analyzed by performing a melting curve analysis. Each reaction had three individual samples in duplicates and values of the threshold cycles were averaged. Relative gene expression was calculated using the $2^{-\text{Ct}}$ method by comparing all of the Ct values to Day 14 control, Collagen–DPSC cultured in DPSC media. Glyceraldehyde-3-phosphate dehydrogenase (GAPDH) was used as the reference gene to normalize target gene expression.

Alkaline Phosphatase Assay.

Osteo/odontogenic differentiation of DPSCs on high-stiffness (800 Pa) oligomeric collagen matrices with and without GF incorporation was quantitatively determined by alkaline phosphatase (ALP) activity on Days 7 and 14, using an ALP assay kit (Sensolyte pNPP). The assay is based on the conversion of *p*-nitrophenyl phosphate (pNPP) to *p*-nitrophenol by the enzyme, which is measured spectrophotometrically at 405 nm. Briefly, the cells encapsulated in oligomeric collagen matrices ($n = 4$) at a density of 1×10^6 per mL were cultured in DMEM/osteogenic differentiation medium (Lonza) with or without BMP2 for 14 days. On Days 7 and 14, the cells were lysed using lysis buffer containing Triton-X 100 (400 μL), vortexed, and the cell-gel suspension was centrifuged for 10 min at 4 °C. Then, 50 μL of the supernatant was added to each well of a 96-well plate and allowed to react for 15 min

with 50 μL of *p*NPP substrate solution at 37 °C. *p*-Nitrophenol (0–300 ng/mL) was used as the standard. The absorbance of standards and samples was measured at 405 nm. Protein concentrations in the samples were determined using a Pierce assay kit (Thermo Scientific).

Alizarin S Red Staining.

For Alizarin S red staining and quantification (Sciencell), the DPSCs-laden oligomeric collagen matrices (800 Pa) ($n = 4$) were stimulated with DMEM or OSM, with or without BMP2. The cultures were fixed in 3.7% formaldehyde for 30 min, and rinsed with distilled water (three times). Then, Alizarin S staining solution was added and incubated at RT for 20 min. Excess dye was removed by rinsing (four times) with distilled water and images were acquired using an inverted bright-field contrast microscope (Leica). Alizarin was extracted from each sample using 10% acetic acid, transferred to microtubes, vortexed, and incubated at 85 °C for 10 min. After cooling in ice, the cells were centrifuged at 20 000*g* for 15 min and the supernatant (200 μL) was neutralized with 75 μL of NH_4OH . Then, 50 μL of the neutralized solution was transferred to a 96-well plate and the absorbance was measured at 405 nm, using a microplate reader.

Statistical Analysis.

Two-way analyses of variance (ANOVA) followed by Holm-Sidak's multiple comparisons were used to evaluate differences in simulated growth factor release, cell survival, endothelial marker mRNA expression, ALP activity, and Alizarin S Red staining between the groups. The significance level was set at $p < 0.05$.

RESULTS

Effect of Oligomeric Collagen Stiffness on the Morphology and Migration of DPSCs.

As stated earlier, by modulating collagen concentration, we were able to establish two distinct matrix stiffnesses (235 and 800 Pa).¹⁹ Here, DPSCs cultured in Oligomer 235 Pa demonstrated spreading on Day 1 (see Figures 3A₁-A₆). Notably, spreading was enhanced in the presence of VEGF. On Day 3 (Figures 3A₁'-A₆'), DPSCs demonstrated a tubular morphology with profuse spreading when VEGF was supplemented in DPSCM (Figure 3A₃') and EGM (Figure 3A₆'). DPSCs cultured within Oligomer 800 Pa demonstrated decreased spreading (Figures 3B₁-B₆), compared to low-stiffness 235 Pa oligomeric collagen matrices. Cytoplasmic projections were found all around the cell periphery (Figures 3B₁-B₆ and 3B₁'-B₆'), compared to the tubular morphology of cells grown in low-stiffness counterparts. DPSCs cultured in OSM and BMP2 (Figures 3B₅ and 3B₆) showed less pseudopodial processes, likely because of the combined effect of OSM and BMP2 on Day 1. However, by Day 3 (Figures 3B₁'-B₆'), the number of pseudopodial extensions from cells increased and appeared to be similar in all matrices.

DPSCs Proliferation in the Oligomeric Collagen Matrices.

The proliferation of DPSCs was significantly increased for all of the 235 Pa (Figure 4A) and 800 Pa (Figure 4B) oligomeric collagen matrices on Day 14. However, cell proliferation was not significantly different between the control and VEGF-modified matrices at any time

point (Figure 4A). Cell proliferation decreased on Days 14 and 21 in 800 Pa matrices containing BMP2, compared to the other two matrices (Figure 4B).

Simulated Growth Factor Release.

The release of FITC-dextran M_w 20 000 and M_w 40 000 from the oligomeric collagen matrices was continuous for 6 days. However, a burst release was seen for PuraMatrix where the simulatory drugs were released within 48 h (see Figure 5).

Endothelial Differentiation on Low-Stiffness (235 Pa) Oligomeric Collagen Matrices.

Figure 6 shows the expression of endothelial cell (EC) markers on Day 14, even in the absence of GFs. There was an increase in the expression of the EC markers when GFs were added to the media, demonstrating their supplementary effect on DPSCs, along with the biophysical factors. The mRNA transcripts of vWF, VE-Cadherin, and PECAM were observed from Day 14 in DPSCs grown in all matrices including the control matrices cultured in DPSCM. Thereafter, a steady increase in the mRNA levels of EC markers was observed until Day 28 (Figures 6A-F). The cells in VEGF-modified matrices, as well as the control matrices, demonstrated a 4-fold to 5-fold increase in vWF mRNA levels by Day 28 (Figure 6A). Matrices cultured in EGM showed a significant increase when VEGF was added to the media (Figure 6B). VE-Cadherin expression significantly increased 10-, 12-, and 16-fold by Day 28 in control, VEGF-modified, and VEGF added (i.e., supplementation of VEGF in the culture media) matrices, respectively (see Figure 6C). The effect was increased 14-, 25-, and 35-fold, respectively, when the same matrices were cultured in differentiation media (Figure 6D). PECAM expression in VEGF-modified matrices in the control and differentiation media showed a 6-fold increase on Day 21. Moreover, there were 10- and 12-fold increases in PECAM expression, respectively, when cells were grown in VEGF-modified matrices in control and differentiation media (see Figures 6E and 6F). The expression levels of VE-Cadherin were higher, compared to vWF and PECAM in matrices cultured in DPSCM and EGM, and the effect of VEGF incorporation was evident. These results demonstrate that the collagen matrices induced endothelial marker expression when cultured in DPSC media. Surprisingly, the level of marker expression increased even in the absence of endothelial differentiation media (see Figures 6A, 6C, and 6E).

Osteogenic Differentiation on High-Stiffness (800 Pa) Oligomeric Collagen Matrices.

ALP activity was observed in DPSCs cultured in 800 Pa collagen matrices, even in the control media (DPSCM), demonstrating the effect of stiffness on osteogenic differentiation (see Figure 7A). While ALP activity significantly increased on Day 14 in control matrices, in osteogenic differentiation media, ALP activity increased on Day 7 in the presence of BMP2. Alizarin staining also demonstrated the level of mineralization of DPSCs in collagen matrices (see Figure 7B). Mineralized nodules were observed on Day 14 in control collagen matrices (see the inset in Figure 7B). The presence of BMP2 increased mineralization levels in the collagen matrices cultured in DPSCM (see the inset in Figure 7B) and OSM (see the inset in Figure 7B). Significant increases in Alizarin staining in the OSM and BMP2 matrices on Day 21 are shown in Figure 7B.

DISCUSSION

DPSCs were used as candidate cells in this study, because of their proven ability to codifferentiate into odontoblasts and endothelial cells.^{7,10,22,25,26} In detail, stem cells derived from the pulp tissue of exfoliated deciduous teeth (SHEDs) have been shown to differentiate into functional odontoblasts and endothelial cells when seeded into tooth slices and implanted subcutaneously in immunodeficient mice.²⁷

An ideal scaffold is expected to provide sufficient cell attachment and support long-term cell survival.^{28,29} In this study, the proliferation of DPSCs was significantly increased for all of the 235 Pa (Figure 4A) and 800 Pa (Figure 4B) oligomeric collagen matrices on Day 14. However, cell proliferation was not significantly different between the control and VEGF-modified matrices at any time point (Figure 4A). Cell proliferation decreased on Days 14 and 21 in 800 Pa matrices containing BMP2, compared to the other two matrices (Figure 4B). The rate of cell proliferation in the compliant matrix was higher on Days 14 and 21, compared to the stiffer matrix, which could be likely due to the longer time taken by the cells to penetrate stiffer matrices. The effect of stiffness on the cytoskeletal organization and cell shape was also evident on the two matrices; stiffer collagen (800 Pa) decreased the cell spreading and actin fiber organization, while compliant collagen supported the growth of elongated DPSCs. Notably, the addition of VEGF to the culture medium improved the amount of sprouting in 235 Pa matrices but the morphology remained tubular, because of the compliant nature of the matrix. The present findings corroborate with a previous study in which oligomeric collagen matrices were able to guide the formation of a three-dimensional lumenized vessel network by endothelial colony forming cells in vitro,²⁰ and could be made denser to mimic hard tissues.³⁰

In the present investigation, we used oligomeric collagen matrices that can be precisely tuned for specific stiffness to instruct the cells to a specific lineage. Furthermore, this study sought to determine whether the differentiation ability of the DPSCs could be further enhanced by morphogenetic signals that supplement those coming from the host enabling guided stem cell differentiation. Here, BMP2 was added to the matrix to supplement the biophysical factor-induced osteogenic differentiation of DPSCs, because dentin-derived BMP2 has been demonstrated to play a key role in inducing differentiation of dental stem cells into odontoblasts.²² The potent role of VEGF in the angiogenesis of pulp tissue is also well-established.³¹ Thus, we incorporated BMP2 and VEGF into the collagen matrices by adding the growth factors (GFs) to the collagen solution before gelation. The GF is retained in the matrices by adsorption and relies on a physical retention and release process via the natural porosity of the oligomeric collagen matrix. Conversely, Galler and colleagues⁹ incorporated the fibroblast growth factor, the transforming growth factor β 1, and VEGF to a self-assembling peptide hydrogel via heparin binding. Although the addition of heparin in the current study could have improved the affinity toward the growth factors,^{9,32} we did not attempt, it because it could potentially interfere with previously optimized matrix stiffnesses. However, even in the absence of heparin, the model growth factors used herein demonstrated a slow release until Day 6, compared to PuraMatrix, which released the GFs within 48 h. Moreover, the released GFs also enhanced endothelial and osteogenic differentiation. Based on these previous reports, it is plausible that, during regenerative endodontics in clinics,

VEGF-incorporated matrices, as well as, VEGF released by DPSCs could enhance vascularization.

As mentioned previously, matrix stiffness has been shown to specify stem cell lineage.³³ We observed the expression of EC markers on Day 14, even in the absence of GFs. Compliant substrates robustly improved EC commitment of human-induced pluripotent stem cells through VECad, CD31, vWF, and eNOS marker expression, without the addition of small molecules.³⁴ Studies have demonstrated that undifferentiated MSCs grown on polymer gels mimicking the ECM elasticity of a given tissue could induce expression of precursor proteins for the cell type typically present in that tissue in the absence of specific GFs.³⁵ There was an increase in the expression of the EC markers when GFs were added to the media, demonstrating their supplementary effect on DPSCs, along with the biophysical factors. Mullane et al.³¹ demonstrated that the treatment of dental pulp tissue in tooth slices with 50 ng/mL recombinant human VEGF prior to implantation into immunodeficient mice increased pulp microvessel density *in vivo*. VEGF/MEK1/ERK signaling pathway and Wnt/ β -catenin signaling were demonstrated to be key regulators of endothelial differentiation in DPSCs.^{25,26} The mRNA transcripts of vWF, VE-Cadherin, and PECAM were observed from Day 14 in DPSCs grown in all matrices including the control matrices cultured in DPSCM. Thereafter, a steady increase in the mRNA levels of endothelial cell markers was observed until Day 28 (see Figures 6A-F). The cells in VEGF-modified matrices, as well as the control matrices, demonstrated a 4-fold to 5-fold increase in vWF mRNA levels by Day 28 (Figure 6A). Matrices cultured in EGM showed a significant increase when VEGF was added to the media (Figure 6B). VE-Cadherin expression was significantly increased 10-, 12-, and 16-fold by Day 28 in control, VEGF-modified, and VEGF-added (i.e., supplementation of VEGF in the culture media) matrices, respectively (see Figure 6C). The effect was increased 14-, 25-, and 35-fold, respectively, when the same matrices were cultured in differentiation media (Figure 6D). PECAM expression in VEGF-modified matrices in the control and differentiation media showed a 6-fold increase on Day 21. Moreover, there were 10- and 12-fold increases in PECAM expression, respectively, when cells were grown in VEGF-modified matrices in control and differentiation media (see Figures 6E and 6F). The expression levels of VE-Cadherin were higher, compared to vWF and PECAM, in matrices cultured in DPSCM and EGM, and the effect of VEGF incorporation was evident. These results demonstrate that the collagen matrices induced endothelial marker expression when cultured in DPSC media. Surprisingly, the level of marker expression increased even in the absence of endothelial differentiation media (see Figures 6A, 6C, and 6E).

Over the past decade, several approaches have been adopted to induce vascularization and mineralization for dental tissue regeneration. Investigators have demonstrated that a co-culture of DPSCs and HUVECs enhanced the odontogenic/osteogenic potential of DPSCs and vasculogenic capacity of HUVECs in cell–cell contact cultures.³⁶ Moreover, the co-culture of DPSCs and HUVECs in PuraMatrix induced more extracellular matrix, vascularization, and mineralization than the DPSC-monocultures *in vivo*.⁴ In this study, we observed improved osteogenic activity of DPSCs in the oligomeric collagen (800 Pa) matrices following the addition of BMP2. Autogenous transplantation of BMP2-treated pellet culture stimulated reparative dentin formation in canine-amputated pulp.³⁷ Another

study demonstrated that blocking the BMP2 signaling inhibited the expression of odontoblastic differentiation markers by SHED cultured in tooth slice/scaffolds, thus demonstrating the key role of BMP2 in odontogenic differentiation.²² The role of p38 mitogen-activated protein kinase-activated canonical Wnt pathway in BMP2-induced DPSC differentiation has also been elucidated.³⁸ ALP activity was observed in DPSCs cultured in 800 Pa matrices, even in the control media (DPSCM), demonstrating the effect of stiffness on osteogenic differentiation of cells (Figure 7A). While ALP activity significantly increased on Day 14 in the control matrices, in osteogenic differentiation media, ALP activity increased on Day 7 in the presence of BMP2. Alizarin staining also demonstrated the level of mineralization of DPSCs in collagen matrices (Figure 7B). Mineralized nodules could be observed on Day 14 in control collagen matrices (see the inset in Figure 7B). The presence of BMP2 increased mineralization levels in the collagen matrices cultured in DPSCM (see the inset in Figure 7B) and OSM (see the inset in Figure 7B). Significant increases in Alizarin staining in the OSM and BMP2 matrices on Day 21 are shown in Figure 7B. These results demonstrate that (i) the high-stiffness (800 Pa) oligomeric collagen matrices could induce osteogenic differentiation, and (ii) the effect was enhanced when BMP2 was directly incorporated to the matrix.

CONCLUSIONS

In aggregate, the current study shows that the collagen gels with stiffnesses of 235 and 800 Pa demonstrated slow release of simulated growth factors, supported long-term cell survival, and favored differentiation of cells to a specific lineage. The collagen matrices of precise stiffness, 235 and 800 Pa, respectively induced endothelial and osteogenic differentiation, and these effects could be further enhanced by the addition of specific growth factors. Our long-term goal is to develop and optimize unique injectable collagen-fibril matrices for delivery and fate regulation of DPSCs in a spatially oriented fashion to form dentin and vascularized pulp at the appropriate locations within the root canal system. Based on these data, we expect that DPSCs transplantation within a high-stiffness matrix containing BMP2 or within a low-stiffness matrix containing VEGF, when concentrically injected into the root canal system, will lead to dentin and pulp regeneration in the appropriate locations. We believe that this approach will be an effective strategy for dental pulp regeneration with significant translational outcomes. Future studies involving the assessment of vascularization and dentin formation using clinically relevant tooth slice models injected *in vivo* with collagen gels individually and concentrically are warranted.

ACKNOWLEDGMENTS

This work was supported by the National Institute for Dental and Craniofacial Research (NIDCR) of the National Institutes of Health under Award Nos. R01DE026578 and K08DE023552 (to M.C.B.). The content is solely the responsibility of the authors and does not necessarily represent the official views of the National Institutes of Health.

REFERENCES

- (1). Zero DT; Zandona AF; Vail MM; Spolnik KJ Dental caries and pulpal disease. *Dent. Clin. North Am* 2011, 55 (1), 29–46. [PubMed: 21094717]

- (2). Cvek M Prognosis of luxated non-vital maxillary incisors treated with calcium hydroxide and filled with gutta-percha. A retrospective clinical study. *Dent. Traumatol* 1992, 8 (2), 45–55.
- (3). Nakashima M; Iohara K; Murakami M Dental pulp stem cells and regeneration. *Endodontic Topics* 2013, 28 (1), 38–50.
- (4). Dissanayaka WL; Hargreaves KM; Jin L; Samaranyake LP; Zhang C The interplay of dental pulp stem cells and endothelial cells in an injectable peptide hydrogel on angiogenesis and pulp regeneration in vivo. *Tissue Eng., Part A* 2015, 21 (3–4), 550–63. [PubMed: 25203774]
- (5). Athirasala A; Lins F; Tahayeri A; Hinds M; Smith AJ; Sedgley C; Ferracane J; Bertassoni LE A Novel Strategy to Engineer Pre-Vascularized Full-Length Dental Pulp-like Tissue Constructs. *Sci Rep.* 2017, 7 (1), 3323. [PubMed: 28607361]
- (6). Athirasala A; Tahayeri A; Thirivikraman G; Franca CM; Monteiro N; Tran V; Ferracane J; Bertassoni LE A dentin-derived hydrogel bioink for 3D bioprinting of cell laden scaffolds for regenerative dentistry. *Biofabrication* 2018, 10 (2), 024101. [PubMed: 29320372]
- (7). Nakashima M; Iohara K; Murakami M; Nakamura H; Sato Y; Arijji Y; Matsushita K Pulp regeneration by transplantation of dental pulp stem cells in pulpitis: a pilot clinical study. *Stem Cell Res. Ther* 2017, 8 (1), 61. [PubMed: 28279187]
- (8). Song JS; Takimoto K; Jeon M; Vadakekalam J; Ruparel NB; Diogenes A Decellularized Human Dental Pulp as a Scaffold for Regenerative Endodontics. *J. Dent. Res* 2017, 96 (6), 640–646. [PubMed: 28196330]
- (9). Galler KM; Hartgerink JD; Cavender AC; Schmalz G; D'Souza RN A customized self-assembling peptide hydrogel for dental pulp tissue engineering. *Tissue Eng., Part A* 2012, 18 (1–2), 176–84. [PubMed: 21827280]
- (10). Rosa V; Zhang Z; Grande RH; Nor JE Dental pulp tissue engineering in full-length human root canals. *J. Dent. Res* 2013, 92 (11), 970–5. [PubMed: 24056227]
- (11). Sancilio S; Gallorini M; Di Nisio C; Marsich E; Di Pietro R; Schweickl H; Cataldi A Alginate/Hydroxyapatite-Based Nanocomposite Scaffolds for Bone Tissue Engineering Improve Dental Pulp Biomineralization and Differentiation. *Stem Cells Int.* 2018, 2018, 9643721. [PubMed: 30154869]
- (12). Bordini EAF; Cassiano FB; Silva ISP; Usberti FR; Anovazzi G; Pacheco LE; Pansani TN; Leite ML; Hebling J; de Souza Costa CA; Soares DG Synergistic potential of 1 α ,25-dihydroxyvitamin D₃ and calcium–aluminum–chitosan scaffolds with dental pulp cells. *Clin. Oral Investig* 2019, 1–12.
- (13). Fioretti F; Mendoza-Palomares C; Helms M; Al Alam D; Richert L; Arntz Y; Rinckenbach S; Garnier F; Haikel Y; Gangloff SC; Benkirane-Jessel N Nanostructured assemblies for dental application. *ACS Nano* 2010, 4 (6), 3277–87. [PubMed: 20507154]
- (14). Zou H; Wang G; Song F; Shi X Investigation of Human Dental Pulp Cells on a Potential Injectable Poly(lactic-co-glycolic acid) Microsphere Scaffold. *J. Endod* 2017, 43 (5), 745–750. [PubMed: 28292602]
- (15). Prescott RS; Alsanea R; Fayad MI; Johnson BR; Wenckus CS; Hao J; John AS; George A In vivo generation of dental pulp-like tissue by using dental pulp stem cells, a collagen scaffold, and dentin matrix protein 1 after subcutaneous transplantation in mice. *J. Endod* 2008, 34 (4), 421–6. [PubMed: 18358888]
- (16). Suzuki T; Lee CH; Chen M; Zhao W; Fu SY; Qi JJ; Chotkowski G; Eisig SB; Wong A; Mao JJ Induced migration of dental pulp stem cells for in vivo pulp regeneration. *J. Dent. Res* 2011, 90 (8), 1013–8. [PubMed: 21586666]
- (17). Kim H; Prasain N; Vemula S; Ferkowicz MJ; Yoshimoto M; Voytik-Harbin SL; Yoder MC Human platelet lysate improves human cord blood derived ECFC survival and vasculogenesis in three dimensional (3D) collagen matrices. *Microvasc. Res* 2015, 101, 72–81. [PubMed: 26122935]
- (18). Phillips JB; Brown R Micro-structured materials and mechanical cues in 3D collagen gels. *Methods Mol. Biol* 2011, 695, 183–96. [PubMed: 21042973]
- (19). Bailey JL; Critser PJ; Whittington C; Kuske JL; Yoder MC; Voytik-Harbin SL Collagen oligomers modulate physical and biological properties of three-dimensional self-assembled matrices. *Biopolymers* 2011, 95 (2), 77–93. [PubMed: 20740490]

- (20). Whittington CF; Yoder MC; Voytik-Harbin SL Collagen-polymer guidance of vessel network formation and stabilization by endothelial colony forming cells in vitro. *Macromol. Biosci* 2013, 13 (9), 1135–49. [PubMed: 23832790]
- (21). Pankajakshan D; Kansal V; Agrawal DK In vitro differentiation of bone marrow derived porcine mesenchymal stem cells to endothelial cells. *J. Tissue Eng. Regener. Med* 2013, 7 (11), 911–20.
- (22). Casagrande L; Demarco FF; Zhang Z; Araujo FB; Shi S; Nor JE Dentin-derived BMP-2 and odontoblast differentiation. *J. Dent. Res* 2010, 89 (6), 603–8. [PubMed: 20351355]
- (23). Kreger ST; Bell BJ; Bailey J; Stites E; Kuske J; Waisner B; Voytik-Harbin SL Polymerization and matrix physical properties as important design considerations for soluble collagen formulations. *Biopolymers* 2010, 93 (8), 690–707. [PubMed: 20235198]
- (24). ASTM Standard F3089: Standard Guide for Characterization and Standardization of Polymerizable Collagen-based Products and Associated Collagen-cell Interactions. In 2014 ASTM Annual Book of Standards; ASTM International: West Conshohocken, PA, 2014.
- (25). Bento LW; Zhang Z; Imai A; Nor F; Dong Z; Shi S; Araujo FB; Nor JE Endothelial differentiation of SHED requires MEK1/ERK signaling. *J. Dent. Res* 2013, 92 (1), 51–7. [PubMed: 23114032]
- (26). Zhang Z; Nor F; Oh M; Cucco C; Shi S; Nor JE Wnt/beta-Catenin Signaling Determines the Vasculogenic Fate of Postnatal Mesenchymal Stem Cells. *Stem Cells* 2016, 34 (6), 1576–87. [PubMed: 26866635]
- (27). Sakai VT; Zhang Z; Dong Z; Neiva KG; Machado MA; Shi S; Santos CF; Nor JE SHED differentiate into functional odontoblasts and endothelium. *J. Dent. Res* 2010, 89 (8), 791–6. [PubMed: 20395410]
- (28). Albuquerque MT; Valera MC; Nakashima M; Nor JE; Bottino MC Tissue-engineering-based strategies for regenerative endodontics. *J. Dent. Res* 2014, 93 (12), 1222–31. [PubMed: 25201917]
- (29). Bottino MC; Pankajakshan D; Nor JE Advanced Scaffolds for Dental Pulp and Periodontal Regeneration. *Dent. Clin. North Am* 2017, 61 (4), 689–711. [PubMed: 28886764]
- (30). Novak T; Seelbinder B; Twitchell CM; van Donkelaar CC; Voytik-Harbin SL; Neu CP Mechanisms and Microenvironment Investigation of Cellularized High Density Gradient Collagen Matrices via Densification. *Adv. Funct. Mater* 2016, 26 (16), 2617–2628. [PubMed: 27346992]
- (31). Mullane EM; Dong Z; Sedgley CM; Hu JC; Botero TM; Holland GR; Nor JE Effects of VEGF and FGF2 on the revascularization of severed human dental pulps. *J. Dent. Res* 2008, 87 (12), 1144–8. [PubMed: 19029083]
- (32). Zieris A; Chwalek K; Prokoph S; Levental KR; Welzel PB; Freudenberg U; Werner C Dual independent delivery of proangiogenic growth factors from starPEG-heparin hydrogels. *J. Controlled Release* 2011, 156 (1), 28–36.
- (33). Engler AJ; Sen S; Sweeney HL; Discher DE Matrix elasticity directs stem cell lineage specification. *Cell* 2006, 126 (4), 677–89. [PubMed: 16923388]
- (34). Smith Q; Chan XY; Carmo AM; Trempel M; Saunders M; Gerecht S Compliant substratum guides endothelial commitment from human pluripotent stem cells. *Sci. Adv.* 2017, 3 (5), No. e1602883. [PubMed: 28580421]
- (35). Reilly GC; Engler AJ Intrinsic extracellular matrix properties regulate stem cell differentiation. *J. Biomech* 2010, 43 (1), 55–62. [PubMed: 19800626]
- (36). Dissanayaka WL; Zhan X; Zhang C; Hargreaves KM; Jin L; Tong EH Coculture of dental pulp stem cells with endothelial cells enhances osteo-/odontogenic and angiogenic potential in vitro. *J. Endod* 2012, 38 (4), 454–63. [PubMed: 22414829]
- (37). Iohara K; Nakashima M; Ito M; Ishikawa M; Nakasima A; Akamine A Dentin regeneration by dental pulp stem cell therapy with recombinant human bone morphogenetic protein 2. *J. Dent. Res* 2004, 83 (8), 590–5. [PubMed: 15271965]
- (38). Yang J; Ye L; Hui TQ; Yang DM; Huang DM; Zhou XD; Mao JJ; Wang CL Bone morphogenetic protein 2-induced human dental pulp cell differentiation involves p38 mitogen-activated protein kinase-activated canonical WNT pathway. *Int. J. Oral Sci* 2015, 7 (2), 95–102. [PubMed: 26047580]

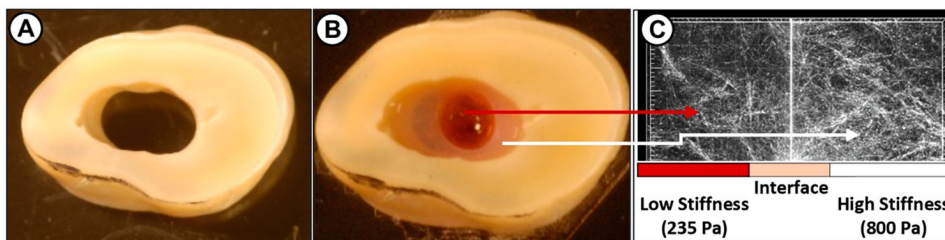


Figure 1.

Schematic illustration of the proposed highly tunable injectable oligomeric collagen-fibril matrix system, using a well-established tooth slice model: (a) tooth slice, (b) concentrically injected collagen matrices (the low-stiffness matrix is purposely dyed in red), and (c) interface adaptation between the two matrices evidenced by reflectance microscopy. For the preparation of concentric collagen matrices, an endodontic fiber post (1.3 mm in diameter, 3MESPE, St. Paul, MN) was placed and stabilized inside the tooth slice. The collagen solution of 2.88 mg/mL (800 Pa) containing DPSC and BMP2 was injected using a needle to the area surrounding the fiber post. Once the matrix is polymerized, the fiber post was lifted and the lumen was injected with a collagen solution (1.37 mg/mL, 235 Pa) containing DPSC and VEGF165 and was allowed to polymerize. The volume ratio of the collagen solutions (1.37 and 2.88 mg/mL) was adjusted to 2:1, which compares with the anatomical features of a root canal. The fibril density and interface adaptation between the two collagen matrices of lower and higher stiffness are shown.


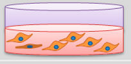
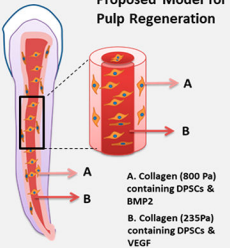
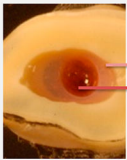









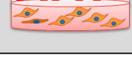
Endothelial Differentiation Culture media/Matrix		Osteogenic Differentiation Culture media/Matrix		Proposed model for future studies
DPSCM/Collagen (235 Pa)		DPSCM/Collagen (800 Pa)		 <p>Proposed Model for Pulp Regeneration</p> <p>A. Collagen (800 Pa) containing DPSCs & BMP2 B. Collagen (235Pa) containing DPSCs & VEGF</p>  <p>Proposed Tooth Slice Model</p>
DPSCM/Collagen (235 Pa) + VEGF		DPSCM/Collagen (800 Pa) + BMP2		
DPSCM/Collagen (235 Pa) + VEGF in media		DPSCM/Collagen (800 Pa) + BMP2 in media		
EGM/Collagen (235 Pa)		OSM/Collagen (800 Pa)		
EGM/Collagen (235 Pa) + VEGF		OSM/Collagen (800 Pa) + BMP2		
EGM/Collagen (235 Pa) + VEGF in media		OSM/Collagen (800 Pa) + BMP2 in media		
VEGF concentration - 50 ng/ml		BMP2 concentration - 50 ng/ml		

Figure 2. Oligomeric collagen matrices and culture media used for endothelial and osteogenic differentiation. The concentric tooth slice model and the dental pulp regeneration model for the future studies are shown.

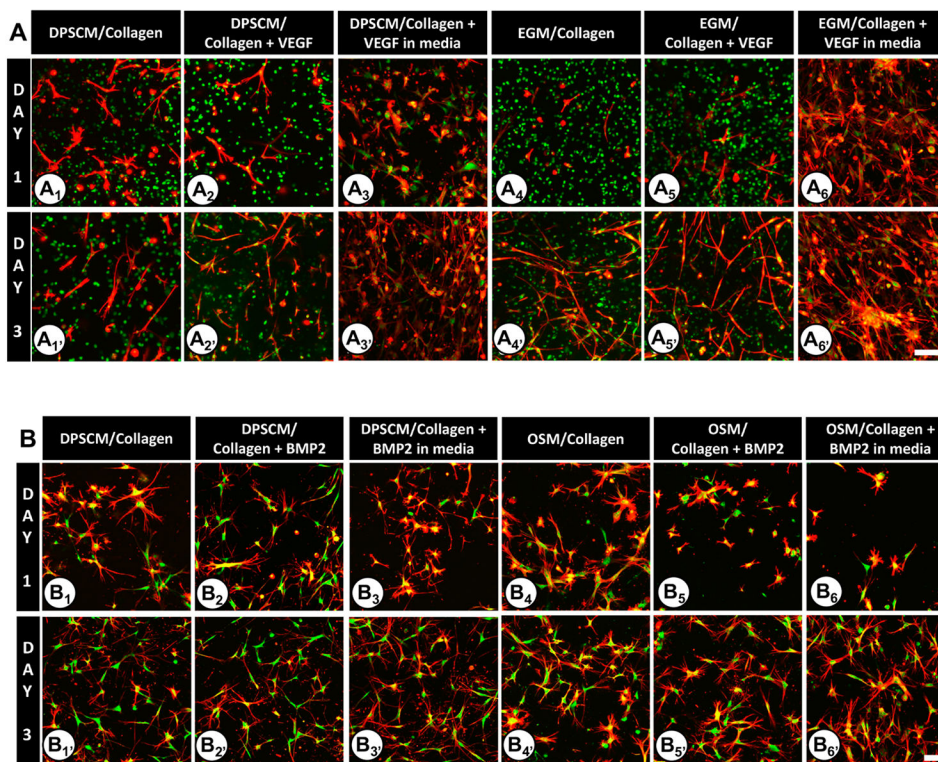


Figure 3.

DPSC adhesion and spreading within Oligomer 235 Pa collagen matrices under various conditions at Days 1 and 3 on the following matrices: (A₁, A₁') DPSCM/collagen; (A₂, A₂') DPSCM/collagen + VEGF; (A₃, A₃') DPSCM/collagen + VEGF in media; (A₄, A₄') EGM/collagen; (A₅, A₅') EGM/collagen + VEGF; (A₆, A₆') EGM/collagen + VEGF in media. DPSC adhesion and spreading within Oligomer 800 Pa collagen matrices under various conditions at Days 1 and 3 on the following matrices: (B₁, B₁') DPSCM/collagen; (B₂, B₂') DPSCM/collagen + BMP2; (B₃, B₃') DPSCM/collagen + BMP2 in media; (B₄, B₄') OSM/collagen; (B₅, B₅') OSM/collagen + BMP2; (B₆, B₆') OSM/collagen + BMP2 in media. For all images, the actin filaments are stained red with rhodamine-phalloidin (excitation and emission at 540/565 nm) and the nucleus is stained green using SYTO 13 (excitation and emission at 488/509 nm). Regions that appear yellow indicate the colocalization of actin and nucleus. Each experiment had three samples. Images are maximum intensity projection of Z-slices (~300 μm depth) captured using a confocal/2-photon Olympus FV1000 MPE system (Olympus America) with a XLUMPLFL20XW objective and 0.95 NA. Scale bar = 100 μm.

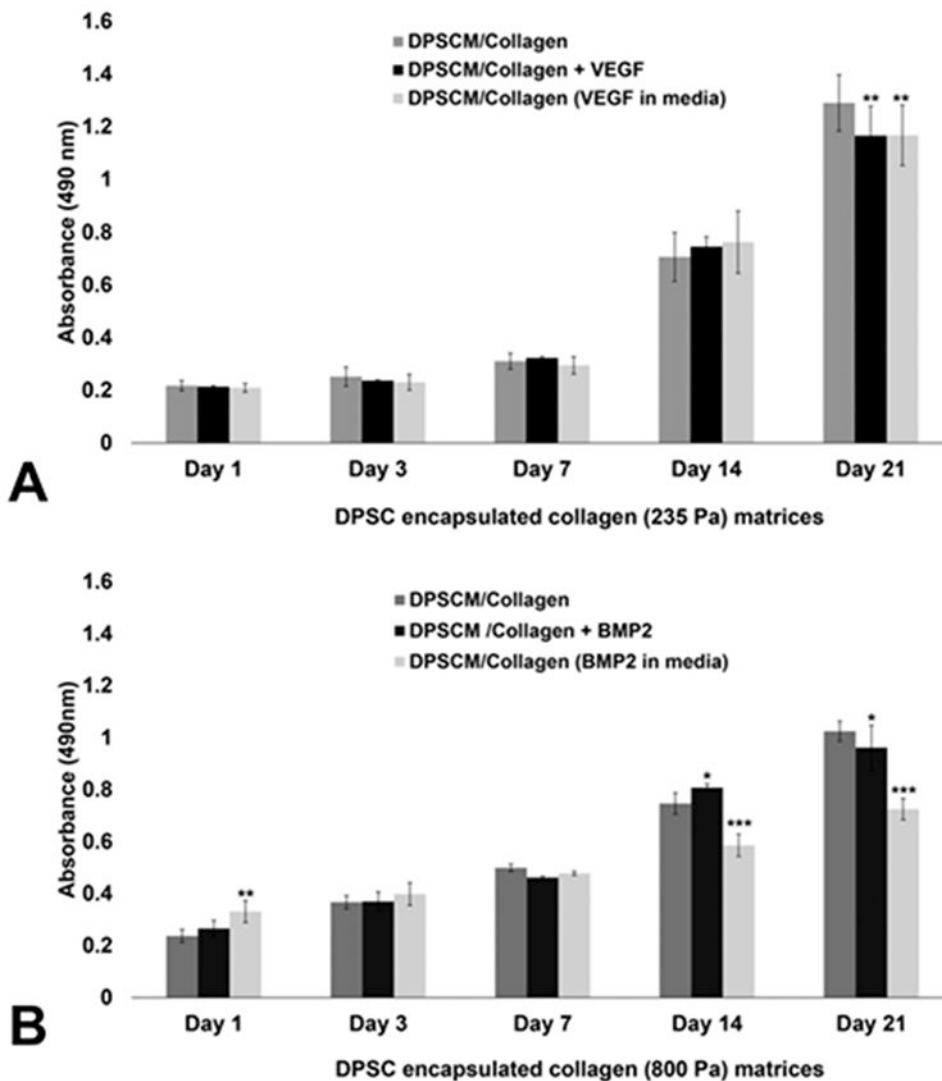


Figure 4. Long-term survival of DPSCs on 235 and 800 Pa collagen matrices: (A) DPSCs survival on 235 Pa collagen matrices on Days 1, 3, 7, 14, and 21 post-encapsulation; and (B) DPSCs survival on 800 Pa collagen matrices on Days 1, 3, 7, 14, and 21 post-encapsulation. The absorbance was read at 490 nm using a microplate reader (Biotek, Winooski, VT, USA). Values represent a mean \pm SD ($n = 3$). [Statistical difference designations: (***) $p < 0.001$, (**) $p < 0.01$, and (*) $p < 0.05$.]

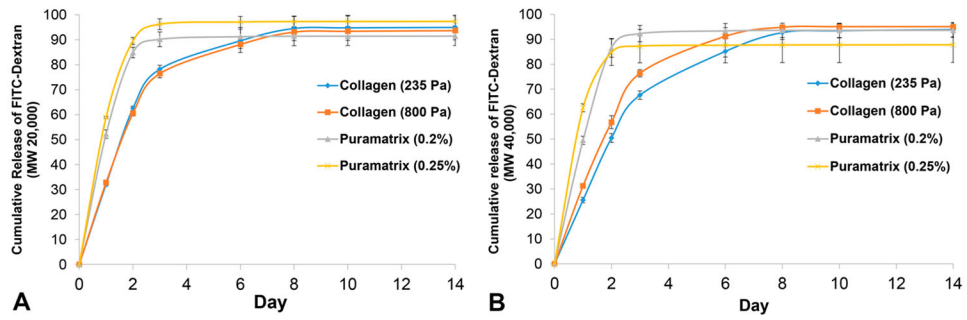


Figure 5. Cumulative release of FITC-Dextran from PuraMatrix and oligomeric collagen matrices for 14 days ($N=5$). FITC-dextran (M_w 20 000 and 40 000) served as model growth factors for (A) BMP2 and (B) VEGF, respectively. Fluorescence intensity was measured (Synergy HTX Microplate Reader, Biotek) using excitation and emission wavelengths of 485 and 520 nm, respectively.

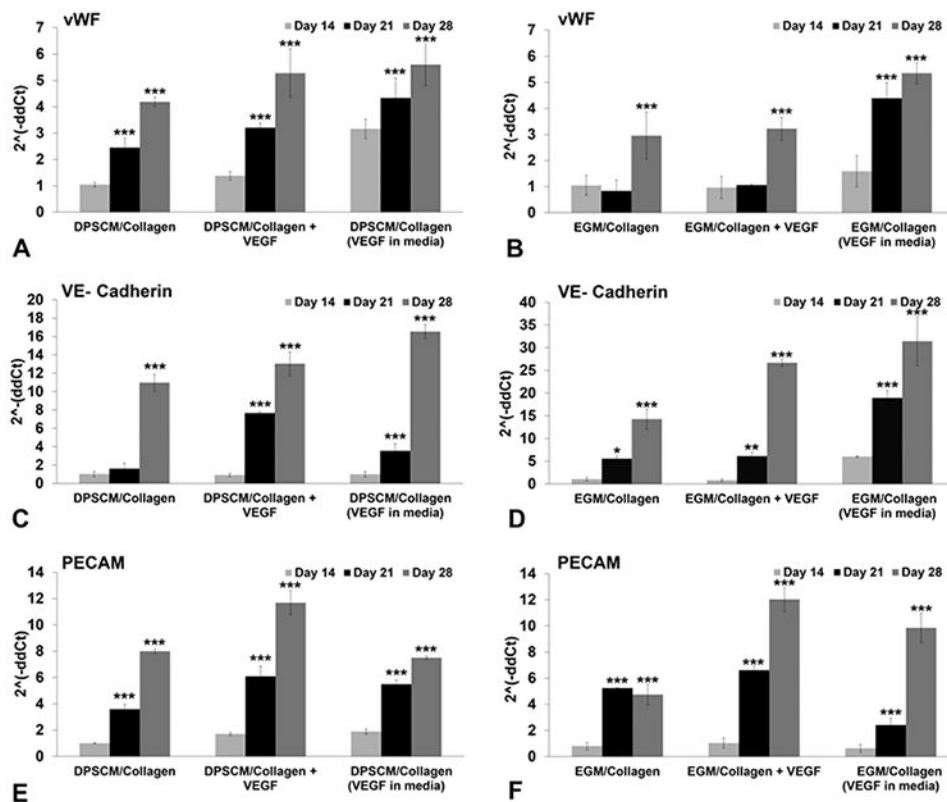


Figure 6. Endothelial differentiation on collagen (235 Pa) matrices. Real-time PCR data (CFX96, Bio-Rad) showing expression levels of endothelial cell markers in DPSCs encapsulated in 235 Pa collagen matrices on Days 14, 21, and 28: (a) vWF–DPSCM, (b) vWF–EGM, (c) VE-Cadherin–DPSCM, (d) VE-Cadherin–EGM, (e) PECAM–DPSCM, and (f) PECAM–EGM. Relative expression of target genes was performed using the 2^{-Ct} method. The results were normalized against the expression of glyceraldehyde-3-phosphate dehydrogenase (GAPDH). Statistical analysis was performed to compare matrices on Days 21 and 28 to Day 14. Values represent the mean \pm SD ($n = 3$). [Statistical difference designations: (***) $p < 0.001$, (**) $p < 0.01$, and (*) $p < 0.05$.]

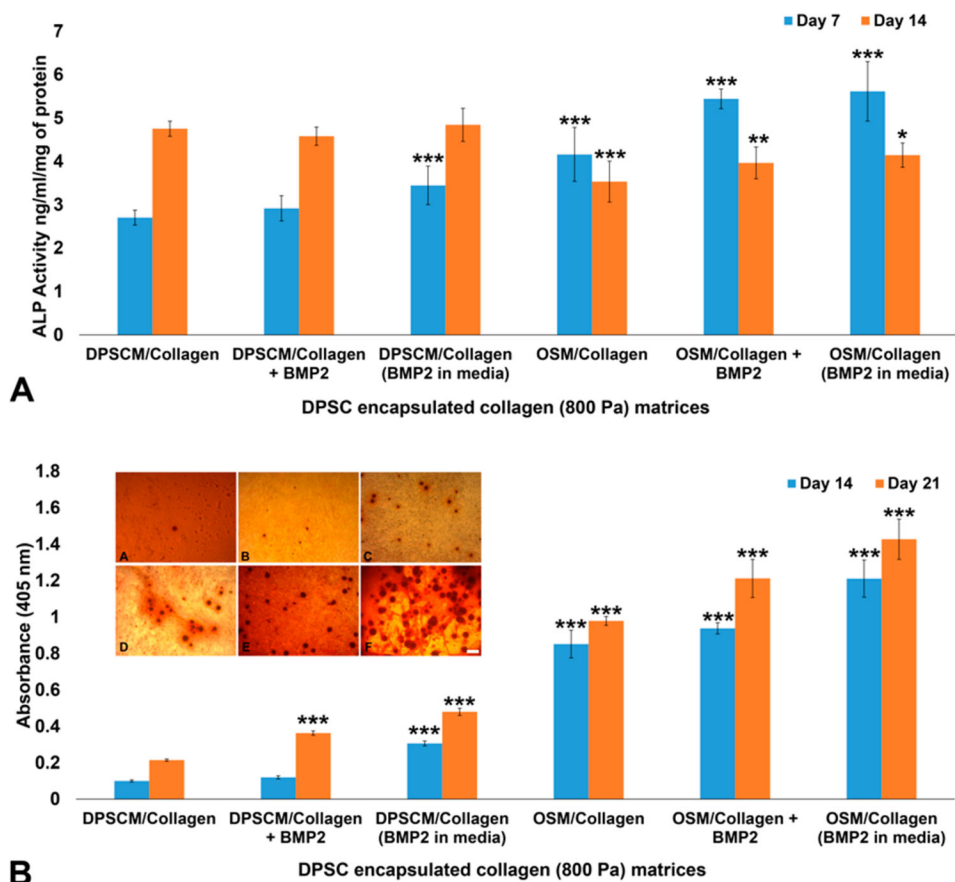


Figure 7. Osteogenic differentiation on collagen (800 Pa) matrices: (A) ALP activity of DPSCs encapsulated in collagen (800 Pa) matrices on Days 7 and 14. The results were normalized to the total protein level and expressed in terms of ng of *p*-nitrophenol produced per mL per μ g protein. Statistical analysis was performed to compare samples to DPSCM/collagen (control) on Days 7 and 14. (B) Alizarin staining of DPSCs encapsulated in collagen (800 Pa) matrices and cultured in DPSCM and OSM for 14 days. Inset shows the bright-field images (Primovert, Zeiss) of Alizarin-stained matrices after 14 days in culture ((micrograph A) DPSCM/collagen, (micrograph B) DPSCM/collagen + BMP2, (micrograph C) DPSCM/collagen + BMP2 in media, (micrograph D) OSM/collagen, (micrograph E) OSM/collagen + BMP2, and (micrograph F) OSM/collagen + BMP2 in media). Values represent mean \pm SD ($n = 4$). [Statistical difference designations: (***) $p < 0.001$, (**) $p < 0.01$, and (*) $p < 0.05$. Scale bar = 50 μ m.]

Table 1.

Primers of Target Genes in RT-PCR

gene	sequence ID	primer sequence	product length (bp)
vWF	NM_000552.4	forward: 5'-ACGTTCTGGTGCAGGATTAC-3' reverse: 5'-GTGACCCGTTTCTTGCATTTC-3'	106
PECAM 1	XM_0111524890.1	forward: 5'-CCGATGTC AAGCTAGGATCATT-3' reverse: 5'-GATGTGGAAC TTGGGTGTAGAG-3'	109
VE-Cadherin	NM_001795.4	forward: 5'-ACCCAAGATGTGGCCCTTTAG-3' reverse: 5'-GTGACACACAGCGAGGTGTAA-3'	100
GAPDH	NM_002046.5	forward: 5'-GGGAAGGTGAAAGGTCGGAGT-3' reverse: 5'-TTGAGGTCAATGAAGGGGTCA-3'	119